Heimo, Juhani; Jokilaakso, Ari; Kekkonen, Marko; Tangstad, Merete; Støre, Anne

Thermal conductivity of titanium slags

Published in:
Metallurgical Research and Technology

DOI:
10.1051/metal/2019064

Published: 01/01/2019

Document Version
Publisher's PDF, also known as Version of record

Metall. Res. Technol. **116**, 635 (2019)

https://doi.org/10.1051/metal/2019064

&Metallurgical Research Technology

Available online at:
www.metallurgical-research.org

Regular Article

Open Access

Thermal conductivity of titanium slags

Juhani Heimo[1], Ari Jokilaakso[1,*], Marko Kekkonen[1], Merete Tangstad[2], and Anne Støre[3]

[1] Aalto University School of Chemical Engineering, Department of Chemical and Metallurgical Engineering, 02150 Espoo, Finland
[2] Norwegian University of Science and Technology, NTNU, 7491 Trondheim, Norway
[3] Metal Production and Processing, SINTEF Industry, 7465 Trondheim, Norway

Received: 2 October 2019 / Accepted: 24 October 2019

Abstract. In ilmenite smelting furnaces, a freeze lining of solidified slag is used to protect the furnace refractories against the aggressive titanium slag. Freeze lining thickness cannot be measured directly due to harshness of conditions inside the process, thus process modelling is required. Several parameters influence the thickness of the freeze-lining, one of them being thermal conductivity of the frozen slag. However, there is a lack of thermal conductivity values for high titanium slags −especially as a function of temperature. In this study, thermal conductivity of three titanium slag samples and an additional sample of freeze-lining was measured from room temperature to 1100/1400 °C with the laser flash analysis method. In addition, thermal expansion and microstructures of the samples were studied to provide an extensive understanding of how microstructure will affect thermal conductivity. The thermal conductivity of the slag samples was found to increase from 1.2 to a maximum of 2.4 W/(m K) when increasing temperature from room temperature to 1100 °C. An additional experiment at 1400 °C showed that the thermal conductivity increased further as the temperature increased. The freeze-lining sample behaves differently, with conductivity being the highest at room temperature, 2.2 W/(m K).

Keywords: freeze lining / ilmenite smelting / laser flash analysis

1 Introduction

Titanium is the ninth most abundant element in the earth's crust, occurring in the mineable forms of ilmenite ($FeTiO_3$) and rutile (TiO_2). Rutile is the less common of the two, with a global production of 850,000 tons in 2015, whereas the global production of ilmenite reached 7.23 million tons in 2015 [1]. The majority of rutile is used in the production of welding rods and titanium metal [2] while ilmenite is mainly used to produce $Ti0_2$-based pigments. The largest pigment producing countries are China and the United States. In 2018, China's pigment production capacity was 3.25 million tons, and the United States' 1.37 million tons [3].

The two predominant processes for titanium dioxide pigment production are the sulphate process and the chloride process. Both processes can utilize high-titanium slag as their raw material [4]. High-titanium slag can be produced by smelting ilmenite concentrate together with a carbonaceous reductant such as anthracite in an electric arc furnace (EAF). The EAF process produces a high-titanium slag and pig iron. The slag is corrosive to refractory materials, and hence ilmenite smelters operate with a freeze lining of solidified slag [5]. Because of the importance of the freeze lining to successful smelter operation, it must be monitored and controlled in order to maintain a safe freeze lining thickness [6]. Freeze lining thickness cannot be measured directly due to harshness of conditions inside the process, thus process modelling is required. Computer modeling of the process can help understand the governing mechanisms of the process and freeze-lining formation, but requires accurate information on slag properties. Several parameters influence the thickness of the freeze-lining, one of them being thermal conductivity of the frozen slag, which directly influences the formation of the freeze-lining on the furnace walls. Accurate knowledge of the thermal conductivity of the ilmenite slag is thus essential for process control, and can improve the quality of simulations that are used to study the smelting process. The thermal conductivity of slag is also an important parameter in the design of furnace-systems based on freeze-lining technology. However, there is a lack of thermal conductivity values for TiO_2-slag, and thus the goal of this research work was to determine the thermal conductivity of ilmenite smelter slag as a function of temperature.

* e-mail: ari.jokilaakso@aalto.fi

Metallurgical slag is typically based on a silicate – oxide mixtures that float on top of a molten metal phase. They have a variety of functions, including impurity control and protecting the melt from oxidation. The slag in the ilmenite smelting process differs from more traditional silicate slags in that it is the primary product of the process, rather than a side-product or waste.

The factors that govern the properties of silicate slags are somewhat different compared to high-TiO_2 slag created in ilmenite smelting operations. The degree of polymerization is the principal factor affecting properties such as the viscosity, electrical conductivity, diffusion coefficient, and thermal conductivity. As one of the most important thermophysical properties, the thermal conductivity of molten slag has been the subject of intensive investigations during the past few decades. The heat conductivity research seems to have been focused mainly on studying silicate-based slags. These studies reveal a tendency for the thermal conductivity to increase as the SiO_2 content increases, suggesting that the silicate structure strongly affects the heat transfer mechanism [7–9]. However, the level of polymerization in the melt is not as important a factor in determining these properties of an ilmenite slag. The structure of TiO_2-rich slags in EAF smelting operations is drastically different from traditional silicate slags. There are no fluxing additions due to very low impurity tolerances, and the main constituents of the slag originate from the ilmenite feed. The slag composition is typically dominated by titanium oxides (85% TiO_2+-Ti_2O_3), with some FeO (10%) and impurities (the remaining 5%). Once solidified, the slag can be viewed as a solid solution of pseudobrookite (M_3O_5) stoichiometry, with titanium existing as Ti_3O_5 and $FeTi_2O_5$, and impurities existing in forms such as $MnTi_2O_5$, $MgTi_2O_5$, Al_2TiO_5 and Cr_2TiO_5 [5].

No experimental results on the measurement of thermal conductivity of high-TiO_2 slag was found in the literature. Due to lack of data, constant thermal conductivity value of 1 W/(m K) for freeze-lining [10] as well as for solid and liquid slag [6] has been assumed in the modelling calculations. Only one article that contains thermal conductivity values for titanium slags as a function of temperature was found. Kotzé and Pistorius [11] developed a heat transfer model for high titanium slag blocks and calibrated their modelling results against thermocouple measurements from pilot-scale titanium slag ingots by adjusting the slag thermal conductivity. The fitted values of the thermal conductivity of the slag was found to increase from approximately 1 to 3 W/(m K), when increasing temperature from 200 to 1500 °C.

Although no measured values of thermal conductivity of high-TiO_2 slag was found, thermal diffusivity of pseudobrookite-type titanates Fe_2TiO_5 and $MgTi_2O_5$ (present in high titanium-slags) has been measured [12,13]. In both studies, thermal diffusivity was found to decrease first and then increase with increasing temperature. This behavior was explained to be a result of closure or healing of the microcracks with increasing temperature.

Viscosity of molten TiO_2-slag is not clearly dependent on temperature, as is with siliceous slags. Instead, the titanium-slag stays very fluid as long as it is fully molten.

Table 1. Chemical analyses for experimental samples.

Species	X2	R2	K19
TiO_2eqv	90.57	77.06	87.60
Ti_2O_3	39.48	16.36	33.62
FeO	3.22	10.03	8.07
Fe_m	0.11	0.30	0.44
MgO	2.55	4.78	1.39
Al_2O_3	1.91	2.14	1.61
CaO	0.25	0.57	0.10
TiO_2	46.70	58.88	50.21
V_2O_3	0.25	0.43	0.28[a]
Cr_2O_3	0.45	0.15	0.14
MnO	1.10	0.31	1.49
SiO_2	1.04	1.72	0.84

[a] Analyzed as V_2O_5.

High-TiO_2 slags have been found to have lower electrical resistivity than siliceous slags, with increasing TiO_2 content bringing forth increasing specific electrical conductivity. The differences in behavior is likely caused by the structures of the slags. According to Handfield and Charette [14], melts rich in TiO_2 easily crystallize and are structurally different from the polymerizing silicate melts.

The electrical conductivity of high-titanium slags is much higher than their siliceous counterparts, reaching 6500 S/m [15]. The specific electrical conductivity of an Al_2O_3-CaO-MgO-SiO_2 quaternary slag systems with varying compositions have been studied by multiple authors [16]. The compiled results at 1500 °C report conductivities as low as 0.8 S/m and high as 63 S/m.

As mentioned earlier, there is lack of thermal conductivity values for TiO_2-slag – especially as a function of temperature. In this study, thermal conductivity of three titanium slag samples and an additional sample of freeze-lining is measured as a function of temperature with the laser flash analysis (LFA) method. In addition, thermal expansion behavior of the samples are presented and microstructures of the samples are studied to provide an extensive understanding of how microstructure will affect thermal conductivity.

2 Experimental work

2.1 Materials

The experimental materials were a selection of process slags (X2, R2 and K19) and an excavated freeze-lining (T1). To obtain proper slag samples for the experiments, slag samples X2 and R2 were remelted in a molybdenum crucible under argon atmosphere at 1600–1750 °C. Slags were allowed to cool with the furnace and samples were drilled form the solidified slag using a diamond drill. The slag K19 did not need to be remelted and the slag samples were drilled directly from a larger process slag piece. Chemical analyses of the samples are shown in Table 1. The analyses were performed by X-ray fluorescence, with titration to determine the proportion of trivalent titanium

in the slag. Sample T1 was not analyzed for chemical composition. Sample X2 has a high TiO_2-equivalent content and represents an ilmenite slag with high purity and high degree of FeO reduction. Sample K19 has a high TiO_2-equivalent content, and higher FeO-content than X2, but lower amount of impurities. Sample R2 has a higher amount of impurities than either of the other slag samples, and notably, a much lower degree of reduction of TiO_2 to Ti_2O_3.

3 Experimental apparatuses and procedure

3.1 Dilatometry

It is essential for thermal conductivity measurement to know how the thickness of the sample changes as a function of temperature. Thus, before the thermal conductivity measurements, thermal expansion characteristics of the materials were determined using Netzsch 402E (NETZSCH-Gerätebau GmbH, Selb, Germany) pushrod dilatometer. Rod-shaped samples of max 8 mm diameter and 10–20 mm length were used in the experiments. The sample was mounted horizontally in a sample holder located inside a furnace. The measurements were done in argon atmosphere and the temperature was increased from room temperature to 1150 °C with a constant heating rate of 2 °C/min. Thermal expansion of the sample during heating was detected by the displacement transducer, which the pushrod was connected to.

3.2 Laser flash analysis

In this study, the laser-flash method was utilized to determine the thermal conductivity of the samples as a function of temperature. The laser flash method was developed by Parker et al. in 1961 [17]. Since then, the method has been subject to extensive development and it is nowadays commonly used technique for the measurement of thermal diffusivity, specific heat capacity and thermal conductivity of various kinds of solids and liquids.

In the laser flash method, the surface of a small, usually disc shape sample is heated by a short energy pulse, sent from the laser. An infrared detector measures the temperature rise on the opposite surface of the sample versus time. Thermal diffusivity (α) can then be determined from the temperature versus time curve and the specific heat capacity (Cp) is calculated comparing the results from the test sample with the results from a well-known reference measured under the same conditions and using the same parameters for both materials. When the bulk density (ρ) of a specimen is known, the thermal conductivity (λ) can be computed according to the following equation:

$$\lambda(T) = \alpha(T) \cdot C_p(T) \cdot \rho(T), \quad (1)$$

where

λ is the thermal conductivity (W/(m K))
α is the thermal diffusivity (m^2/s)
Cp is the specific heat capacity (J/(kg K))
ρ is the density (kg/m^3)

In this study, the LFA experiments were conducted in two stages. The first stage, measuring conductivities between room temperature and 1100 °C, took place at SINTEF in Trondheim, Norway, using a Netzsch LFA 457 instrument (Netzsch-Gerätebau GmbH in Selb, Germany). The measurements were done in nitrogen atmosphere and the temperature was increased from room temperature to 1100 °C with a constant heating rate of 100 °C/30 min. For experiments closer to the melting point of the slags, measurements were carried out in Netzsch-Gerätebau GmbH in Selb, Germany, using their LFA 427 instrument and argon atmosphere. The limitations of the experimental setup led to the reduction of the measurements to one temperature point (1400 °C) for a single sample (X2).

A core drill core with the required diameter of 12.7 mm was used in the determination of the thermal conductivity. Discs with approximately 2 mm thickness were prepared with a low speed saw. These slices were dried in a furnace at 120 °C to ensure evaporation of any left-over moisture from the drilling and sawing processes. Some of the samples had an appreciable amount of porosity, and large surface pores needed to be covered to ensure that the samples had an even thickness. The thickness of the sample is very important in the determination of the thermal diffusivity. If the laser beam hits the bottom of a large pore the heat obtained will have shorter distance to travel through the sample and will subsequently result in too high diffusivity values. A paste mixture of fine silicon carbide powder and water was used to fill the pores to achieve a flat surface. Ideally only the outer surface of the pores should be covered leaving the pore underneath open, but this is difficult to achieve. Once a sample had a flat surface on both circular faces, thin layers of graphite were sprayed on both surfaces. Both the smoothness and blackness of the surface were necessary to ensure the quality of the result of the laser flash experiments. For the measurements of sample material X2 at Netzsch, a disc of 12.6 mm diameter was used, and a single sample of approximately 4 mm thickness was used.

4 Results and discussion

4.1 Thermal expansion

The results obtained by the dilatometry measurements are presented in Figure 1. As can be seen, the thermal expansion curve of slag type K19 follows a similar trend as slag sample X2, increasing and decreasing in particular temperature ranges. The composition of the samples are close to each other, thus similar behavior during heating was expected. Samples R2 and T1 shows almost linear expansion with increasing temperature. Slag type R2 has different chemical composition (higher FeO-, TiO_2-, MgO- and SiO_2-content) compared to slag types K19 and X2, but it needs systematic study of thermal expansion characteristics in relation to chemical composition before definite conclusions can be drawn from the main influencing factor. This was, however, not within the scope of this study. In all cases, the thermal expansion was low, below 1% from room temperature to 1150 °C. Low thermal expansion is attributed presumably to the fact that expansion mainly fills the gaps of the grain boundary cracks, which are

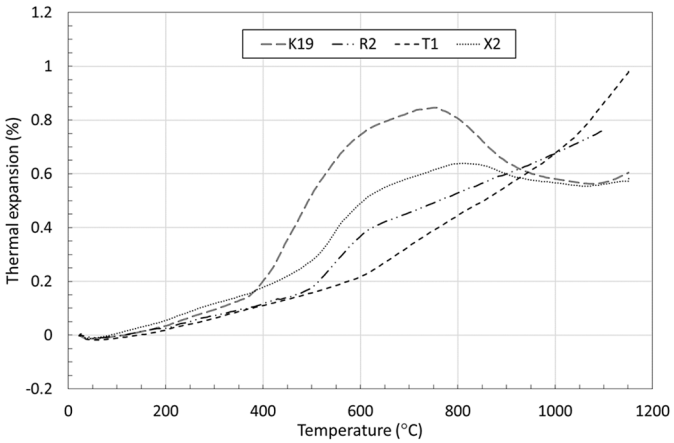

Fig. 1. Thermal expansion of the studied materials.

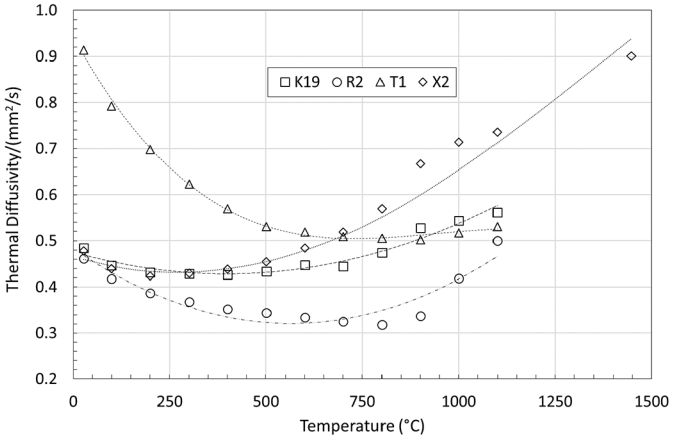

Fig. 3. Combined thermal diffusivity data from LFA analysis of samples K19, R2, X2 and T1 (trend lines for visual support).

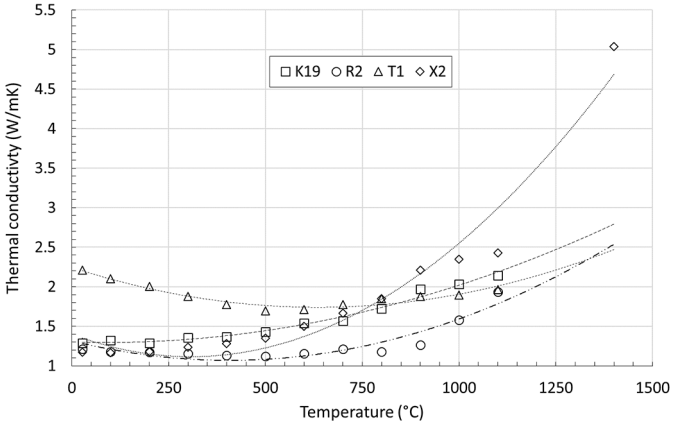

Fig. 2. Combined thermal conductivity data from LFA analysis of samples K19, R2, X2 and T1 (trend lines for visual support).

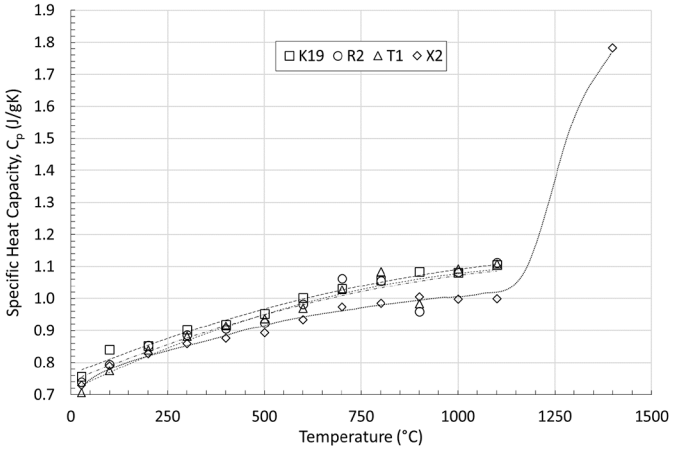

Fig. 4. Combined specific heat capacity data from LFA analysis of samples K19, R2, X2 and T1 (trend lines for visual support).

typical for solidified high-titanium slags (Figs. 5–9). The results from the thermal expansion measurements were used in the calculation of densities of the samples, which are needed when computing thermal conductivities.

4.2 Thermal conductivity

Four materials were analyzed with LFA. Two to three samples from each material were measured. Samples were heated from room temperature to 1100 °C in nitrogen atmosphere and measurements were taken at 100 °C intervals. Three measurements were made for each sample at each temperature. Additionally, sample X2 was analyzed separately at 1400 °C with three measurements. The results were averaged and plotted over the temperature range. The combined results of all materials are presented in Figure 2.

Thermal conductivity of the slag samples increased from approximately 1.2 to a maximum of 2.4 W/(m K) when increasing temperature from room temperature to 1100 °C. Sample X2 was additionally tested at 1400 °C, where thermal conductivity of 5 W/(m K) was obtained, which means that the thermal conductivity continued to rise by increasing temperature. Based on this result, it may be predicted that the other slags may also behave similarly, but more measurements are needed to confirm this.

Slag samples K19 and X2 behaves similarly during heating; thermal conductivity stayed relatively stable until 400 °C and then started to increase with temperature. In the case of slag sample R2, thermal conductivity stayed stable until 800 °C and then began to increase significantly with temperature. The increase in temperature seems to have a greater impact on the thermal conductivity of slags X2 and R2 than on slag K19, which displays more linear relationship between temperature and thermal conductivity. The freeze-lining sample T1 behaves differently than the other materials, with conductivity being the highest at room temperature (2.2 W/(m K)) and linearly decreasing to 1.7 W/(m K) with increasing temperature until about 500 °C. After that, the thermal conductivity increased with temperature.

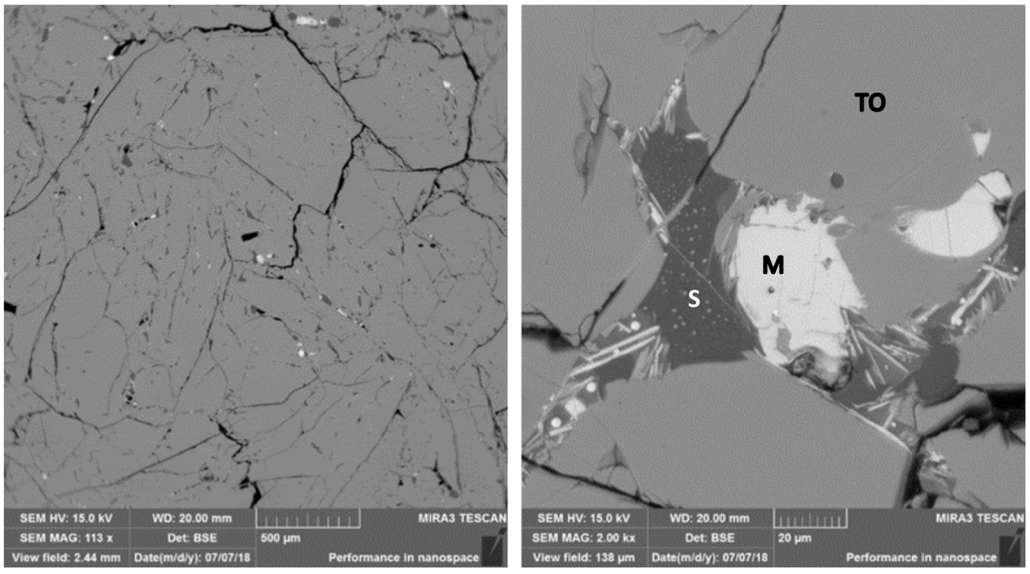

Fig. 5. Microstructure of slag sample K19; backscattered electron images of the same field at two different magnifications. The light grey areas are titanium-rich oxides (labelled TO), the dark-grey areas are silicates (labelled S), the white areas are metals (labelled M) and the black areas are pores.

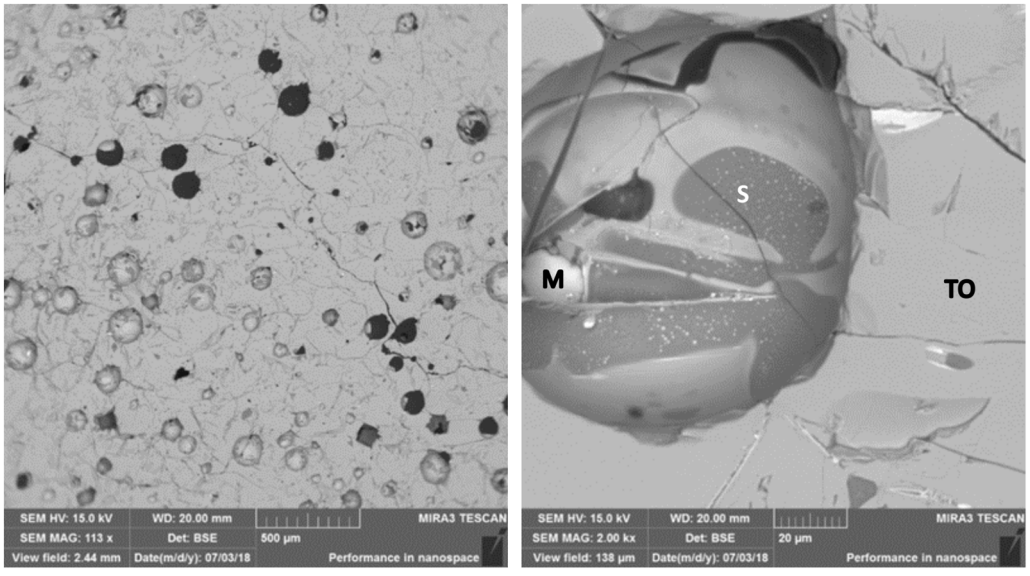

Fig. 6. Microstructure of slag sample X2; backscattered electron images of the same field at two different magnifications. The light grey areas are titanium-rich oxides (labelled TO), the dark-grey areas are silicates (labelled S), the white areas are metals (labelled M) and the black areas are pores.

The measured thermal conductivity values are higher than 1 W/(m K), which has been used previously in modelling calculations [6,10], but they are in line with the values reported by Kotzé and Pistorius [11].

4.3 Thermal diffusivity and specific heat capacity

The other two quantities in equation (1) were also measured and their results are presented in Figures 3 and 4. The thermal diffusivity behaves as a function of temperature in a similar way as the thermal conductivity as they are closely related. The values are between 0.3–0.9 mm^2/s (0.3–0.9 $10^{-6}\,m^2/s$) which correspond value for fused silica (0.834), but are less than that for polycrystalline titanium dioxide (2.8) [18].

The specific heat capacity values were very close to each other in all studied materials, between 700–1100 J/(kg K). They are also close to the literature values of silicon dioxide (745) and titanium dioxide (710) [18]. Sample X2 was additionally tested at 1400 °C, where specific heat capacity of 1800 J/(kg K) was obtained.

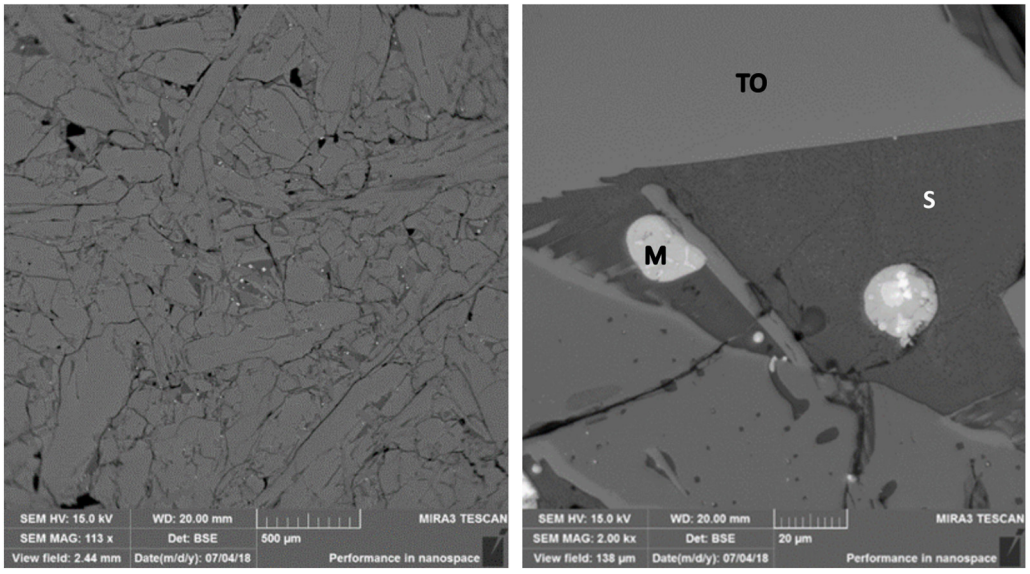

Fig. 7. Microstructure of slag sample R2; backscattered electron images of the same field at two different magnifications. The light grey areas are titanium-rich oxides (labelled TO), the dark-grey areas are silicates (labelled S), the white areas are metals (labelled M) and the black areas are pores.

4.4 Characterization of the samples

After the experiments, microstructure of the samples were examined by Scanning electron microscope (SEM) for analysing the amount of voids, cracks or other discontinuities present in the samples during the LFA measurement. Energy-dispersive X-ray spectroscopy (EDS) was used for element analysis in the phases present in the samples.

Figures 5–9 illustrate the microstructures of slag samples K19, R2 and X2 as well as freeze-lining sample T1 after the experiments. The microstructure of the samples is dominated by a titanium rich oxide phase, containing varying amounts of iron and magnesium. The other phases present are a silicate phase and metallic phase containing mainly iron. The glassy silicate phase contains most of the impurities of the slag like aluminium and calcium, and is found mainly between the titanium-rich oxide grains. The metallic iron particles are present as globules inside the silicate grains. The phase structure of the samples is in agreement with the previous studies [15,19,20].

In addition, the microstructures of the slag samples displayed substantial microcracking. This is typical to solidified titanium slags since all pseudobrookite-type titanates, such as Al_2TiO_5, $MgTi_2O_5$ and Fe_2TiO_5 are characterized by a strong expansion anisotropy [21]. Internal cracks formed by thermal stresses are one likely reason for the relatively low thermal conductivity of the samples at low temperature. At elevated temperatures, slag samples exhibited increased thermal conductivity, which could, therefore, be attributed to microcrack closure [12,13], but confirming this will require further studies.

Although the compositions of the slag samples K19 and X2 are close to each other, the slag structures are clearly different. The pores in sample K19 are mainly long cracks. Some of the smaller cracks are partially filled with silicates. Conversely, the cracks in X2 appear much smaller although more numerous, and the main pores are circular in shape. The X2 slag was remelted to facilitate sample preparation, and some bubbling was reported to have occurred in the crucible. This bubbling is the likely cause of these spherical pores. Another noteworthy characteristic of the bubbles is that most of the metallic and glassy constituents of the sample seem to be concentrated inside these pores. The longer and wider cracks evident in the K19 sample are creating sharper discontinuities in the material than the spherical pores in X2. Although the depth of the cracks and overall prevalence of either of these structural faults cannot be fully assessed from the SEM images, it seems that the nominal degree of porosity does not have such a high impact on thermal conductivity as the nature of the pores. Microcracks appear to be more effective than spherical pores in lowering the thermal conductivity, and thus represent a significant barrier to heat flow. This argument is strengthened somewhat by the measured results, as X2 reaches a higher conductivity than K19.

Lattice vibrations can propagate around spherical pores equally well from all directions, but cracks can impede their movement more. The vibrations must find a route around the cracks, but depending on the direction of the propagation, the distance required can be much longer in relation to the absolute size of the crack. Furthermore, as is evident in the SEM images, the cracks in these materials are not parallel.

The behavior of sample R2 was slightly different from the other two slags, as the thermal conductivity did not immediately begin to rise with the increase in temperature. This may be due to the microstructure of the sample. Comparison of SEM images shows that R2 has more microcracks and probably due to this smaller grain size

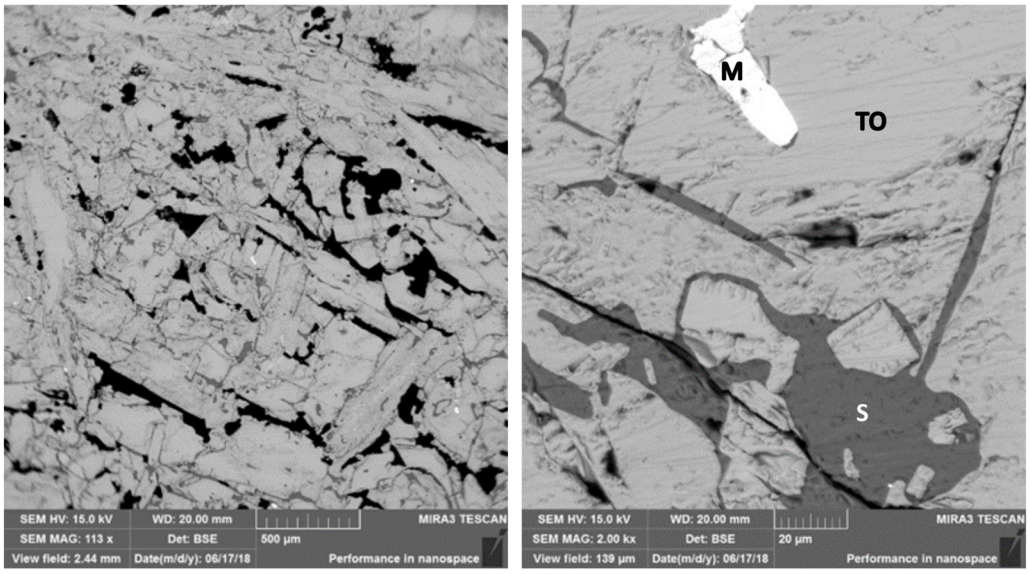

Fig. 8. Microstructure of freeze-lining sample T1; backscattered electron images of the same field at two different magnifications. The light grey areas are titanium-rich oxides (labelled TO), the dark-grey areas are silicates (labelled S), the white areas are metals (labelled M) and the black areas are pores.

than the slag samples K19 and X2. Since cracks and grain boundaries impede lattice vibration, this structural factor may be the cause of the lower thermal conductivity of R2 throughout the temperature range.

Sample T1 differs from the three other samples as it is a piece of excavated freeze-lining. Although the chemical composition of the freeze-lining sample was not analyzed, its composition was expected to differ from the composition of tapped slag. The reasons for this include the observed entrainment of larger metal droplets in the freeze-lining, as well as the partial dissolution of the refractory material to the freeze-lining. Samples for the LFA measurements were prepared from a section of the sample material that did not contain large metal droplets. However, computed tomography (CT) scan from the LFA freeze-lining sample T1 (Fig. 9) shows a localized concentration of metal droplets. The structure appears to have a crystalline nature, with lamellar formations of the main oxide matrix, and high porosity.

The results of the LFA measurements showed differences in behavior between the slag (X2, R2 and K19) and freeze-lining (T1) samples. At room temperature, the thermal conductivity of the freeze-lining sample is approximately double to that of the other samples and begins to decrease as temperature is increased. Iron metal has a thermal conductivity of around 80 W/(m K) at room temperature [18], which is in a different order of magnitude than the measured conductivities in this work. It can be speculated that the relatively high thermal conductivity of iron contributes to the conductivity of the freeze-lining material, which appears to contain more metallic iron than the slag samples. Furthermore, the thermal conductivity of iron is inversely proportional to temperature, as is shown in Figure 10. This could explain why the thermal conductivity of the sample decreases with increasing temperature up to about 500 °C. The subsequent increase in thermal conductivity with increasing temperature could then be explained by the characteristic behavior of the titanium bearing oxide matrix that makes up most of the sample, as the thermal conductivity of the small amount of iron in the material continues to decrease. However, to confirm this speculation, a series of thermal conductivity measurements of samples with measured volume fractions of the iron droplets must be carried out. Higher thermal conductivity of the freeze-lining sample T1 at low temperatures could also be due to the fact that it has more crystalline structure than the slag samples.

Each sample exhibited a degree of porosity, although the types of pores varied. The effect of macroscale porosity on the bulk thermal conductivity of the tested materials could not be determined, because the LFA method utilized very small samples. However, the fact that both the excavated freeze-lining and the slag samples had some degree of pores would indicate that freeze-linings in ilmenite smelting is also porous. Thereby, it could be assumed that the real thermal conductivity values of a freeze-lining could be different from what the slag itself might suggest.

The effect of freeze-lining formation on the heat flux through the furnace wall depends on the thermal conductivity of the freeze-lining. For example, MgO refractories have a thermal conductivity between 4.5 and 6.5 W/(m K) in 1000 °C according to prior research [22,23], with an inverse relationship to temperature. The results of this investigation suggest that Pistorius's estimate of 1 W/(m K) thermal conductivity for the smelter freeze-lining [10] may need re-evaluation, and the heat flux from the bath through the layers of the furnace wall is greater than estimated. From an industrial standpoint, these more accurate results enable more realistic results of thermal design, process optimization and simulation.

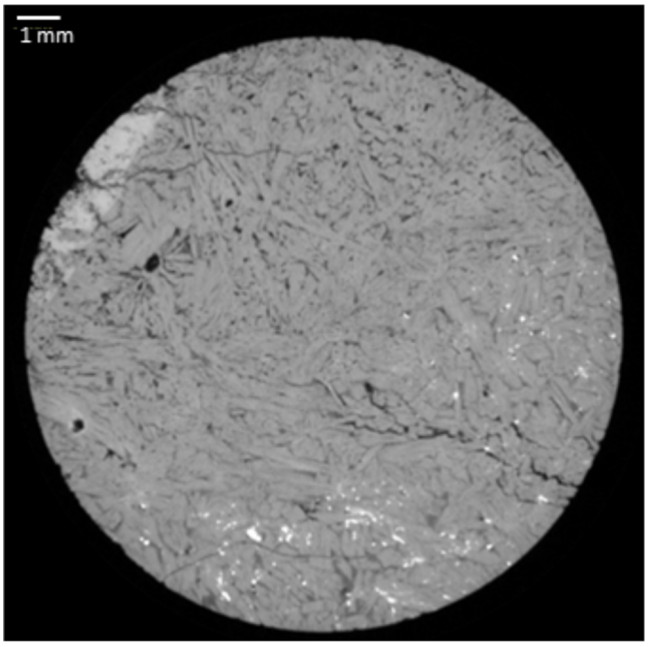

Fig. 9. CT image of freeze-lining sample T1.

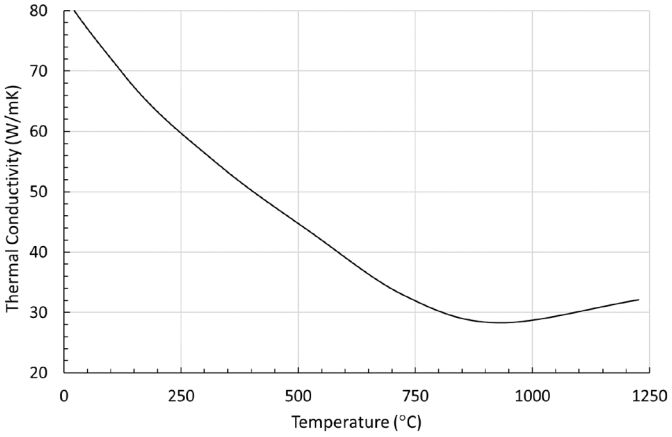

Fig. 10. Thermal conductivity (W/[m K]) of the pure iron as a function of temperature (data from [18]).

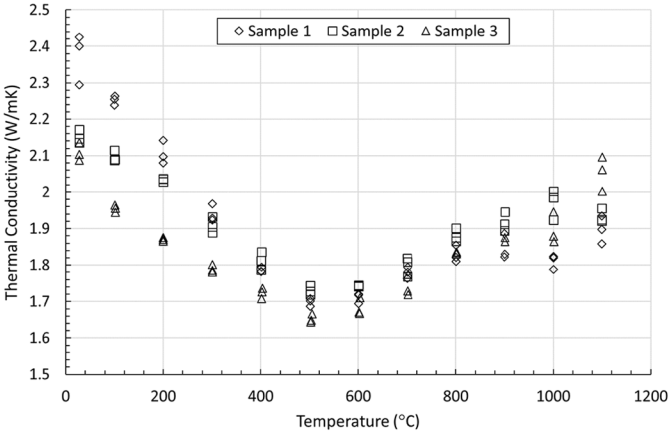

Fig. 11. Repeat measurements of sample T1.

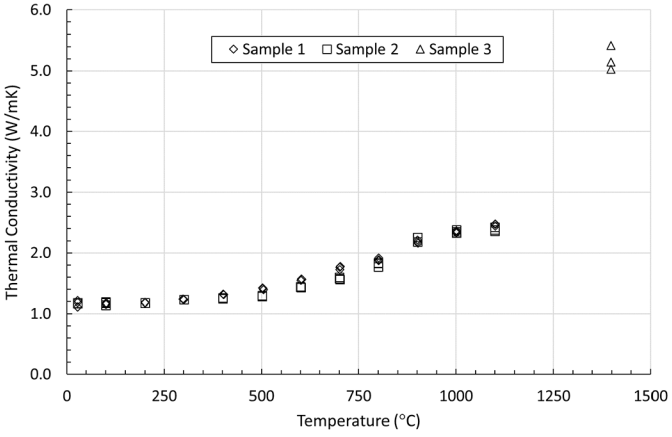

Fig. 12. Repeat measurements of sample X2.

5 Error analysis of experimental results

Thermal conductivity measurements on both solid and liquid slags are known to contain contributions from radiation and convection. In Netzsch LFA 427 and 457 Laser flash analysers radiative and convective heat loss corrections are integrated in data analysis software. According to the manufacturer, the accuracy in measuring thermal diffusivity is ±3% and heat capacity ±5% [24]. The LFA measurement results from room temperature to 1100 °C for sample T1 are presented in Figure 11. The material exhibits good repeatability of measurements. The disparity between repeated measurements is generally smaller than the difference between samples, which implies the precision of the LFA measurements. The samples behave fairly similarly throughout the measured temperature range.

The repeatability of the LFA measurements from room temperature to 1100 °C for slag X2 are validated with samples 1 and 2 results in Figure 12. Repeated measurements of the thermal conductivity of each sample are reasonably close to each other. Samples 1 and 2 behave highly similarly throughout the measured temperature range. Sample 3 was sent to Netzsch for measurement at 1400 °C. Also in this case, the measurements showed good reproducibility.

The measured values for thermal conductivity from room temperature to 1100 °C for samples R2 and K19 are shown in Figures 13 and 14 below, respectively. Overall, there is more divergence in the results, but the repeatability is acceptable although, especially on the higher end of the temperature spectrum, there is an increased spread, peaking at 1100 °C, suggesting need for more carefulness when using the values for high temperature conditions.

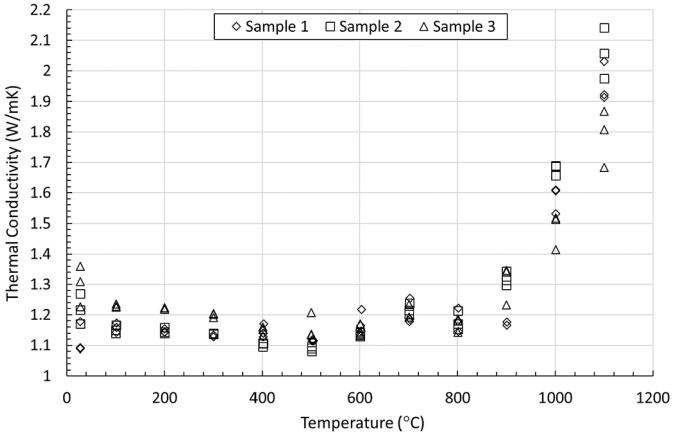

Fig. 13. Repeat measurements of sample R2.

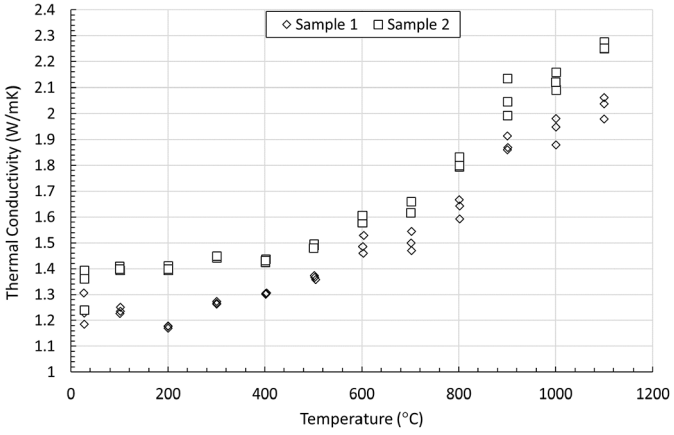

Fig. 14. Repeat measurements of sample K19.

6 Conclusions

The key material property of freeze-lining in ilmenite smelting furnace walls is the thermal conductivity of the high-titanium slag. Most of the available thermal conductivity data are for silicate-based slag systems, so there is a lack of thermal conductivity values for high titanium slags −especially as a function of temperature. Accurate knowledge of the thermal conductivity of the titanium slag is essential for modeling, design and control of the ilmenite smelting process.

In ilmenite smelting process, a safe freeze lining thickness must be maintained due to aggressive nature of the slag against refractory material. Since there are no direct means to measure the thickness of the freeze lining layer, process modelling is required. The success of such models to predict freeze lining formation is highly dependent on the thermophysical property data used in the simulations.

In this study, thermal conductivity of three titanium slag samples and an additional sample of freeze-lining was measured from room temperature to 1100 °C/1400 °C with the laser flash analysis method. The thermal conductivity of the slags appeared to increase with temperature. The freeze-lining sample behaves differently, with conductivity being the highest at room temperature. This may be due to small metallic particles present in the sample. All measurements showed consistent results with good reproducibility.

The microstructure of the samples was dominated by a titanium rich oxide phase. The other phases present were a silicate phase and metallic phase containing mainly iron. Moreover, microcracks appear to be more effective than spherical pores in lowering the thermal conductivity, and thus represent a significant barrier to heat flow. The slag samples in this study displayed substantial microcracking, which is one likely reason for the relatively low thermal conductivity of the samples at low temperature, but confirming this will require further studies with pre- and post-microstructural characterization of the samples.

Acknowledgments. This study has been supported by TEKES (Business Finland) financed project FLEX (grant number 8155/31/2016) and partly financed by Outotec (Finland) Oy, and made use of the Academy of Finland's RawMatTERS Finland Infrastructure (RAMI), based jointly at Aalto University, GTK Espoo and VTT Espoo. The experimental work done by Yngvar Andersen and Tor-Eivind Ebbesen from NTNU as part of their BSc theses as well as one slag sample from SFI Metal Production, is greatly acknowledged.

References

1. G.M. Bedinger, 2015 Minerals Yearbook, Titanium (advance release), U.S. Geological Survey, 2018
2. W. Zhang, Z. Zhu, C.Y. Cheng, A literature review of titanium metallurgical processes, Hydrometallurgy **108**, 177 (2011)
3. Mineral Commodity Summaries 2019, U.S. Geological Survey, 2019
4. K.K. Sahu, T.C. Alex, D. Mishra, A. Agrawal, An overview on the production of pigment grade titania from titania-rich slag, Waste Manage. Res. **24**, 74 (2006)
5. P.C. Pistorius, Ilmenite smelting: the basics, J. South Afr. Inst. Min. Metall. **108**, 35 (2008)
6. J.H. Zietsman, P.C. Pistorius, Ilmenite smelter freeze lining monitoring by thermocouple measurements: model results, in: M. Akser, J. Elder (Eds.), Heavy minerals conference proceedings, society for mining, metallurgy and exploration Inc. 2005, pp. 221–228
7. Y. Kang, J. Lee, K. Morita, Thermal conductivity of molten slags: a review of measurement techniques and discussion based on microstructural analysis, ISIJ Int. **54**, 2008 (2014)
8. Y. Kang, K. Morita, Thermal conductivity of the CaO–Al_2O_3–SiO_2 system, ISIJ Int. **46**, 420 (2006)
9. K.C. Mills, The influence of structure on the physico-chemical properties of slags, ISIJ Intl. **33**, 148 (1993)
10. P.C. Pistorius, Equilibrium interactions between freeze lining and slag in ilmenite smelting, J. South Afr. Inst. Min. Metall. **104**, 417 (2004)
11. H. Kotzé, P.C. Pistorius, A heat transfer model for high titania slag blocks, J. South Afr. Inst. Min. Metall. **110**, 57 (2010)
12. H.J. Siebeneck, D.P.H. Hasselman, J.J. Cleveland, R.C. Bradt, Effect of microcracking on the thermal diffusivity of Fe_2TiO_5, J. Am. Ceram. Soc. **59**, 241 (1976)

13. H.J. Siebeneck, D.P.H. Hasselman, J.J. Cleveland, R.C. Bradt, Effects of grain size and microcracking on the thermal diffusivity of $MgTi_2O_5$, J. Am. Ceram. Soc. **60**, 336 (1977)
14. G. Handfield, G.G. Charette, Viscosity and structure of industrial high TiO_2 slags, Can. Metall. Q. **10**, 235 (1971)
15. M. Guéguin, F. Cardarelli, Chemistry and mineralogy of titania-rich slags. Part 1–hemo-ilmenite, sulphate and upgraded titania slags, Miner. Process. Extr. Metall. Rev. **28**, 1 (2007)
16. Slag Atlas, 2nd edition, Verlag Stahleisen GmbH, Dusseldorf, 1995
17. W.J. Parker, R.J. Jenkins, C.P. Butler, G.L. Abbott, Flash method of determining thermal diffusivity, heat capacity, and thermal conductivity, J. Appl. Phys. **32**, 1679 (1961)
18. F.P. Incropera, D.P. DeWitt (eds.), Fundamentals of heat and mass transfer, 4th edition, John Wiley & Sons, New York, 1996
19. P.C. Pistorius, C. Coetzee, Physicochemical aspects of titanium slag production and solidification, Metall. Mater. Trans. B. **34B**, 581 (2003)
20. R.H. Stana, Solidification of titanium slags and influence on post processing, Master thesis, Norwegian University of Science and Technology, 2016
21. G. Bayer, Thermal expansion characteristics and stability of pseudobrookite-type compounds Me_3O_5, J. Less-Common Met. **24**, 129 (1971)
22. S. Min, J. Blumm, A. Lindemann, A new laser flash system for measurement of the thermophysical properties, Thermochim. Acta **455**, 46 (2007)
23. Y. Saito, K. Kanematsu, T. Matsui, Measurement of thermal conductivity of magnesia brick with straight brick specimens by hot wire method, Mater. Trans. **50**, 2623 (2009)
24. NETZSCH-Gerätebau GmbH. www.netzsch.com

Cite this article as: Juhani Heimo, Ari Jokilaakso, Marko Kekkonen, Merete Tangstad, Anne Støre, Thermal conductivity of titanium slags, Metall. Res. Technol. **116**, 635 (2019)